

Connexin43 Associated with an N-cadherin-containing Multiprotein Complex Is Required for Gap Junction Formation in NIH3T3 Cells*

Received for publication, November 15, 2004, and in revised form, February 23, 2005
Published, JBC Papers in Press, February 28, 2005, DOI 10.1074/jbc.M412921200

Chih-Jen Wei, Richard Francis, Xin Xu, and Cecilia W. Lo‡

From the Laboratory of Developmental Biology, NHLBI, National Institutes of Health, Department of Health and Human Services, Bethesda, Maryland 20892

Previous studies have indicated an intimate linkage between gap junction and adherens junction formation. It was suggested this could reflect the close membrane-membrane apposition required for junction formation. In NIH3T3 cells, we observed the colocalization of connexin43 (Cx43 α 1) gap junction protein with N-cadherin, p120, and other N-cadherin-associated proteins at regions of cell-cell contact. We also found that Cx43 α 1, N-cadherin, and N-cadherin-associated proteins were coimmunoprecipitated by antibodies to either Cx43 α 1, N-cadherin, or various N-cadherin-associated proteins. These findings suggest that Cx43 α 1 and N-cadherin are coassembled in a multiprotein complex containing various N-cadherin-associated proteins. Studies using siRNA knockdown indicated that cell surface expression of Cx43 α 1 required N-cadherin, and conversely, N-cadherin cell surface expression required Cx43 α 1. Pulse-chase labeling and cell surface biotinylation experiments indicated that in the absence of N-cadherin, Cx43 α 1 cell surface trafficking is blocked. Surprisingly, siRNA knockdown of p120, an N-cadherin-associated protein known to modulate cell surface turnover of N-cadherin, reduced N-cadherin cell surface expression without altering Cx43 α 1 expression. These observations suggest that in contrast to the coregulated cell surface trafficking of Cx43 α 1 and N-cadherin, N-cadherin turnover at the cell surface may be regulated independently of Cx43 α 1. Functional studies showed gap junctional communication is reduced and cell motility inhibited with N-cadherin or Cx43 α 1 knockdown, consistent with the observed loss of both gap junction and cadherin contacts with either knockdown. Overall, these studies indicate that the intracellular coassembly of connexin and cadherin is required for gap junction and adherens junction formation, a process that likely underlies the intimate association between gap junction and adherens junction formation.

Gap junctions are specialized cell junctions containing hydrophilic channels that mediate intercellular communication. They play an essential role in electrical and metabolic coupling by regulating the movement of ions and small molecules between cells (1). Gap junctions are comprised of two hemichannels, each consisting of a hexameric assembly of transmem-

brane proteins known as the connexins (2). In the mouse genome, there are 20 connexin genes and each generate gap junction channels with different gating and regulatory properties that are likely dictated by the intracellular domains of the proteins (3).

The gap junction gene, *Gja1*, is one of the most widely expressed connexin genes. It encodes a 43-kDa protein known as connexin43 or α_1 connexin, referred to here as Cx43 α 1.¹ Cx43 α 1 is synthesized in the endoplasmic reticulum and transported to the trans-Golgi network, where it is oligomerized (4). This is followed by trafficking to the cell surface and incorporation of the hexameric arrays into gap junction plaques at regions of cell-cell contact (5). The Cx43 α 1 protein has a half-life of only 1–5 h (for review, see Ref. 6), and is turned over through the endosomal/lysosomal pathway (7–9). The cytoplasmic terminus (CT) of Cx43 α 1 is subject to modification by a variety of protein kinases (10, 11). In Western blots, there is typically a faster migrating species of Cx43 α 1 that co-migrates with nonphosphorylated Cx43 α 1 (NP), and one or more slower migrating bands containing phosphorylated isoforms. The NP form is intracellular, whereas the phosphorylated P2 form is localized in gap junction plaques (12–14).

Various studies have indicated that gap junction formation is dependent on the assembly of adherens junctions. This was first indicated by studies in which antibody-mediated disruption of cadherin-containing cell adhesion contacts were shown to block gap junction formation (15–17). More recent studies showed that N-cadherin knockout cardiomyocytes are Cx43 α 1 gap junction-deficient (18), whereas expression of a dominant-negative N-cadherin construct in cardiomyocytes was shown to disrupt Cx43 α 1 gap junctions (19). A reciprocal requirement for gap junctions in adherens junction formation also has been noted. For example, when gap junction antibodies were injected into 2-cell mouse embryos, the embryos failed to undergo compaction, a process regulated by cadherins (20). In *Xenopus* embryos, expression of a dominant negative Cx32 β 1/Cx43 α 1 chimeric construct inhibited gap junction communication, and led to the extrusion of cells from the embryo because of a loss of cell adhesion contacts (21). In another study, treatment of cells with Fab fragments targeting Cx43 α 1 or Cx32 β 1 blocked both gap junction as well as adherens junction formation (17). Together these findings indicate that formation of gap junction and adherens junction are intimately linked. It was previously suggested that this might reflect the close membrane-membrane apposition required for gap junction and adherens junction formation (17).

We previously showed that Cx43 α 1 gap junctions also can

* This work was supported by National Institutes of Health Grant Z01-HL005701. The costs of publication of this article were defrayed in part by the payment of page charges. This article must therefore be hereby marked "advertisement" in accordance with 18 U.S.C. Section 1734 solely to indicate this fact.

‡ To whom correspondence should be addressed: 50 South Dr. MSC 8019, Rm. 4537, Bethesda, MD 20892-8019. Tel.: 301-451-8041; Fax: 301-480-4581; E-mail: loc@nhlbi.nih.gov.

¹ The abbreviations used are: Cx43 α 1, connexin43; N-cadherin, neuronal cadherin; p120, p120-catenin; siRNA, small interfering RNA; GST, glutathione S-transferase; FITC, fluorescein isothiocyanate; CT, cytoplasmic terminus; NP, nonphosphorylated.

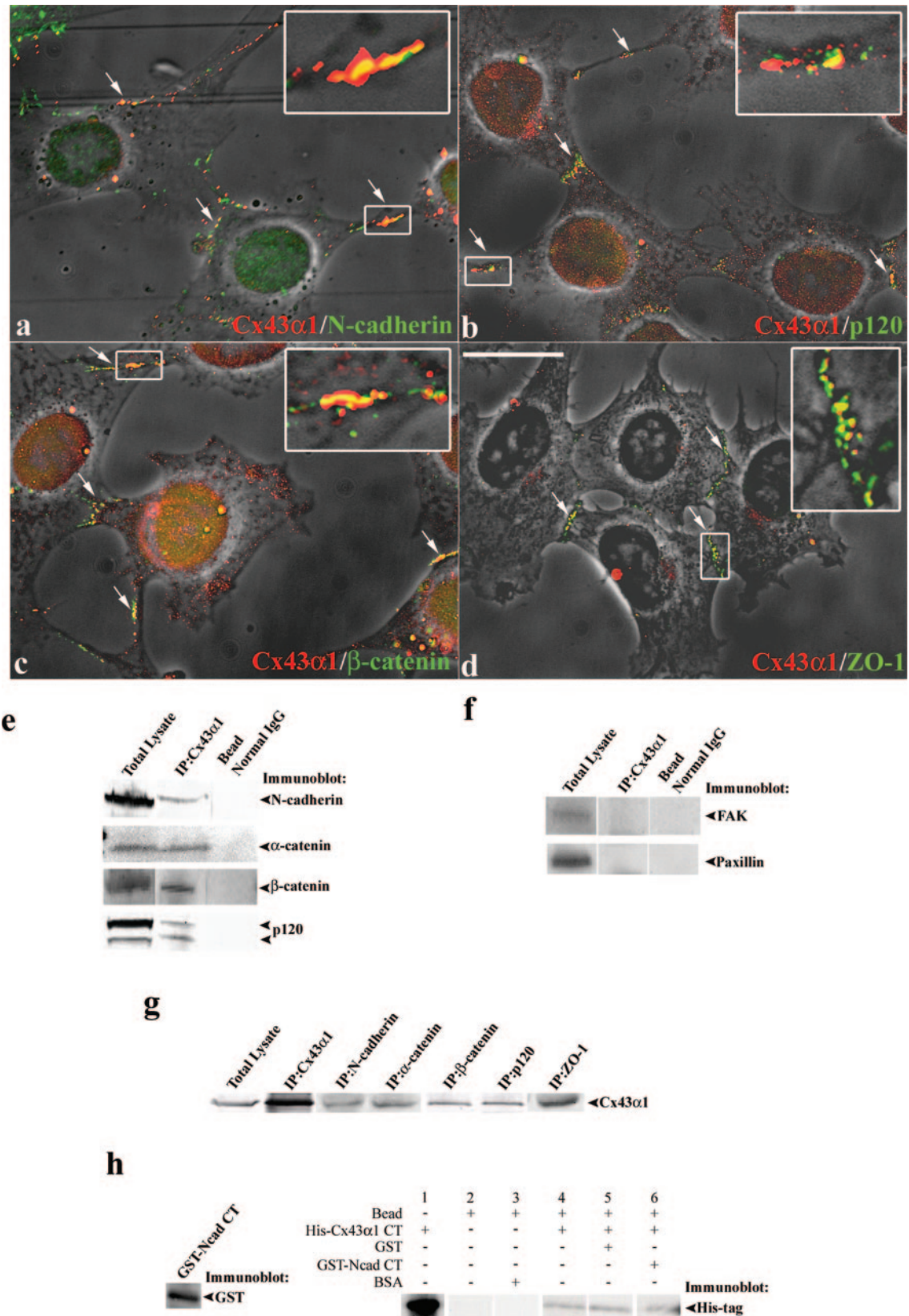


FIG. 1. Cx43 α 1 and N-cadherin protein interactions. Panels *a–d*, double immunostaining of NIH3T3 cells showed at regions of cell-cell contact, colocalization of Cx43 α 1 (red) with other proteins (green) including N-cadherin (panel *a*), p120 (panel *b*), β -catenin (panel *c*), and ZO-1 (panel *d*) (see regions denoted by white arrows). These are merged phase contrast and darkfield immunofluorescence images. Boxed area is shown in magnified view in upper right inset, and corresponds to a region showing Cx43 α 1 colocalization with N-cadherin or N-cadherin-associated protein. Scale bar, 25 μ m. Panel *e*, cell lysates were immunoprecipitated with a Cx43 α 1 antibody, then Western immunoblotted using antibodies to α -catenin, β -catenin, N-cadherin, and p120. With each antibody, a band of the expected size for respective proteins was obtained, showing that N-cadherin and N-cadherin-associated proteins were coimmunoprecipitated with Cx43 α 1. Panel *f*, Cx43 α 1 antibody precipitates analyzed by Western immunoblotting using antibodies to paxillin or FAK showed neither of these two proteins was in the Cx43 α 1 immunoprecipitates. Panel *g*, immunoprecipitates obtained from cell lysates incubated with antibodies to either N-cadherin, or various N-cadherin-associated proteins were

modulate cell motility. Thus altered neural crest cell motility was shown to contribute to the cardiac phenotype of the Cx43 α 1 knockout mouse (22–24). We found in migrating neural crest cells, the colocalization of Cx43 α 1 and N-cadherin at many regions of cell-cell contact (24). To further examine the interactions between Cx43 α 1 and N-cadherin, and investigate their role in regulating gap junction communication and cell motility, in this study we used NIH3T3 cells as a model system. NIH3T3 cells are reminiscent of neural crest cells, as they are a highly motile mesenchymal cell type, and express both Cx43 α 1 and N-cadherin. Analyses by immunohistochemistry, and coimmunoprecipitation and Western immunoblotting indicated that Cx43 α 1 and N-cadherin are coassembled in a large multiprotein complex. Consistent with this, siRNA-mediated knockdown of either Cx43 α 1 or N-cadherin resulted in the apparent loss of both proteins from the cell surface. Surface biotinylation and pulse chase experiments showed that cell surface trafficking of Cx43 α 1 is blocked with siRNA-mediated N-cadherin knockdown. However, siRNA knockdown of p120, a N-cadherin-associated protein known to modulate cell surface turnover of N-cadherin (25), eliminated cell surface expression of N-cadherin without affecting Cx43 α 1 expression. This suggests that the cell surface turnover of N-cadherin may be regulated independently of Cx43 α 1. We also found with either N-cadherin or Cx43 α 1 knockdown, not only was gap junctional communication reduced, but cell motility was inhibited. This is consistent with the observed loss of both gap junction and cell adhesion contacts with either knockdown. Overall, these studies indicate that the intracellular coassembly of connexin and cadherin is required for gap junction and adherens junction formation. This process of coassembly likely accounts for the intimate linkage between gap junction and adherens junction formation, a process that is also functionally important in the modulation of cell motility.

EXPERIMENTAL PROCEDURES

Antibodies—Mouse monoclonal Cx43 α 1 antibodies used for coimmunoprecipitation and Western immunoblotting were from Fred Hutchinson Cancer Research Center (P2C4), and from Chemicon. Rabbit polyclonal Cx43 α 1 antibody used for immunoblotting was from Sigma. Rabbit polyclonal Cx43 α 1 antibody (18A-8) used for immunofluorescence microscopy was a generous gift from Dr. Elliot Hertzberg (Albert Einstein College of Medicine). Mouse monoclonal antibodies to N-cadherin, ZO-1, GST, and rabbit polyclonal antibody to ZO-1 were purchased from Zymed Laboratories. Mouse monoclonal antibodies against His tag, β -catenin, p120, N-cadherin, FAK, and paxillin were purchased from BD Biosciences. Rabbit polyclonal antibodies to α - and β -catenin were purchased from Sigma. Secondary antibodies used included mouse monoclonal, horseradish peroxidase-conjugated goat anti-mouse IgG (BD Biosciences), anti-rabbit IgG (Sigma), and FITC- or Cy3-conjugated goat anti-rabbit or anti-mouse antibodies (Jackson ImmunoResearch Laboratories). Normal mouse or rabbit IgG was from Santa Cruz Biotechnology, Inc.

Immunohistochemistry—NIH3T3 cells were fixed with 4% paraformaldehyde for 15 min or 4% paraformaldehyde containing 0.15% Triton X-100 for 10 min, then washed and incubated with primary antibody at 4 °C overnight, followed by incubation in FITC- or Cy3-conjugated secondary antibodies. Epifluorescence was carried out on a Leica DMRE microscope with a $\times 63$ PL oil objective and imaged using an ORCA-ER camera (Hamamatsu). Z stacks comprised of 0.2- μ m optical slices were obtained and deconvolved using Volocity iterative deconvolution algorithm (Improvision, Ltd.). All images shown in this study are derived from merging 3 deconvolved optical sections.

Immunoprecipitation and Western Immunoblotting—NIH3T3 cells

were harvested and lysed in radioimmune precipitation assay buffer (RIPA, 150 mM NaCl, 1% Nonidet P-40, 0.5% sodium deoxycholate, 1 mM EDTA, 0.1% SDS, 50 mM Tris, pH 7.5) containing complete protease inhibitors (no. 8140, Sigma) and 1 mM phenylmethylsulfonyl fluoride for 15 min at 4 °C. Protein concentration was determined by BCA assay (Pierce). Lysates were precleared using protein G-agarose beads (Invitrogen) and centrifuged at 15,000 $\times g$ for 10 min. The supernatants were incubated with desired antibodies (10 μ g) bound to protein G-agarose beads at 4 °C for overnight, washed extensively with cold RIPA buffer, and resolved by SDS-PAGE. The gel was electroblotted and processed for chemiluminescence detection using horseradish peroxidase-conjugated secondary antibodies. For some experiments, cells were treated with the lysosomal inhibitor ammonium chloride (Sigma) for 24 h prior to lysis in RIPA buffer, followed by immunoblotting analysis.

Construction and Purification of His- and GST-tagged Fusion Proteins—To generate His-tagged Cx43 α 1 CT-expressing vector, cDNA encoding the CT domain of Cx43 α 1 (amino acids 227–382) was generated by PCR using primers 5'-CCGGAATTCGCGCTCTTCTATGTCTTCTTC-3' and 5'-CCGCTCGAGTTAAATCTCCAGGTCATCAGGC-3', and ligated into the EcoRI/XhoI sites of pET28a vector (Novagen). The recombinant vector was transformed into *Escherichia coli* BL21(DE3) pLysS, and the fusion protein was purified as previously described (26).

To generate GST-tagged fusion containing the CT domain of N-cadherin (amino acids 753–904), the cDNA for mouse N-cadherin (kindly provided by Dr. Glenn L. Radice, University of Pennsylvania) was PCR-amplified using primers 5'-CCGGAATTCATGCGCCAAGC-CAAGCAGCTTTTAAATTGAC-3' and 5'-CCGCTCGAGTCAGTCGTCAC-CACCGCGTACATGTCCGC-3', and the resulting PCR fragment was inserted into the EcoRI/XhoI sites of pGEX-T4-1 expression vector (Amersham Biosciences). After expression in *E. coli* DH5 α , GST-tagged fusion proteins was purified by affinity chromatography on a glutathione-Sepharose 4B column (Amersham Biosciences).

Affinity Binding Assay—Purified GST-tagged N-cadherin CT (GST-N-cad-CT, bait) was immobilized on glutathione-agarose beads (Pierce), and after extensive washing, was incubated with previously purified His-tagged Cx43 α 1-CT (His-Cx43 α 1-CT, prey) for 2 h at 4 °C. His-Cx43 α 1-CT was also incubated with the glutathione beads as prey control, and GST-glutathione beads were used as bait control. Bound GST or GST-N-cad-CT fusion proteins was eluted in elution buffer (50 mM reduced glutathione, 50 mM Tris-HCl, pH 8.0), and subjected to immunoblot analysis with a GST antibody.

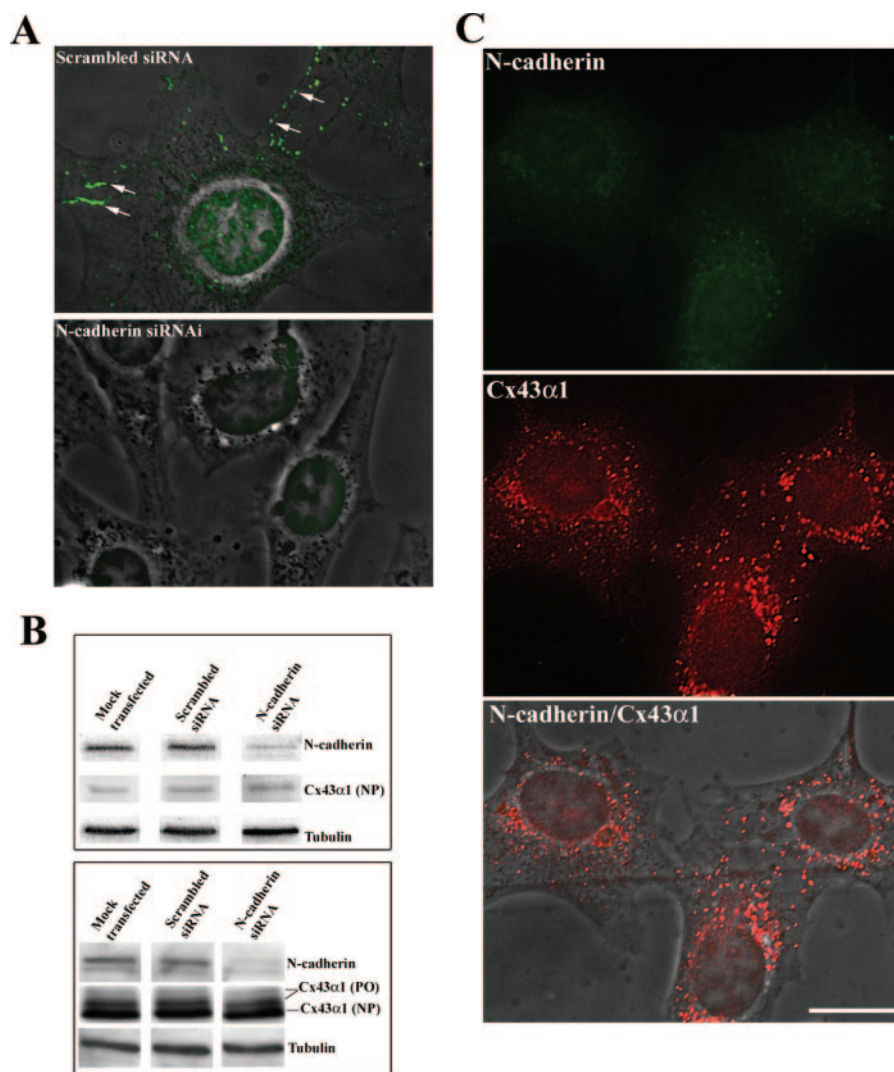
siRNA-mediated Knockdown—For siRNA-mediated knockdown of Cx43 α 1 and N-cadherin, siRNAs (Dharmacon, Inc.) were synthesized containing nucleotides 143–163 (AACAGTCTGCCTTTTCGCTGTA) and 859–879 (AAGCTGGTCACTGGTGACAGA) of the mouse Cx43 α 1 coding sequence, and nucleotides 139–159 (AAGGATGTGCACGAAGGACAG) and 1049–1069 (AAGCCACAGACATGGAAGGCA) of the mouse N-cadherin coding sequence. Scrambled siRNAs contained the same sequences except for 3 mismatched nucleotides (for Cx43 α 1: AACAGTATGCCGTTTCGCCGTA, and AAGCTGTTTCGCTGGGGACAGA; for N-cadherin: AAGGATGGGAACGCAGGACAG, and AAGCCACGGCCAT-AGAAGGCA).

Oligofectamine (Invitrogen) was used to transfect NIH3T3 cells with the siRNAs for immunofluorescence microscopy and Western immunoblotting. For time lapse videomicroscopy, cells were electroporated with siRNAs and a GFP expression vector, pEGFP-C1 (Clontech, Inc.), using Cell Line Nucleofector Kit R (Amaxa Biosystems). Alternatively, siRNA-mediated knockdown was performed using a mammalian expression vector directing intracellular synthesis of siRNA-like transcripts (27). They were made by inserting into pSuper.neo+gfp vector (OligoEngine), an oligonucleotide sequence corresponding to mouse Cx43 α 1 (CAGTCTGCCTTTTCGCTGTA), p120 (CGAAGTATCGCTGAGAAC), or N-cadherin (GCCACAGACATGGAAGGCA). We also generated control plasmids with 3 nucleotide mismatches in the 19-nucleotide targeting sequences.

Dye Coupling Assay—NIH3T3 cells were co-transfected with Cx43 α 1 or N-cadherin siRNAs and a pDsRed2-N1 expression vector (Clontech, Inc.), and used 48 h after transfection. Prior to microelectrode impale-

analyzed by Western immunoblotting using a Cx43 α 1 antibody. Cx43 α 1 was observed in all of these immunoprecipitates. *Panel h*, affinity pull-down assays were carried out using purified GST-N-cad-CT bound to glutathione beads as bait (*left panel*). These were incubated with purified His-Cx43 α 1-CT, which served as prey (*right panel, lane 1*). Bait-prey interaction was examined by immunoblotting proteins pulled down by the bait-loaded beads using a His tag antibody. Controls included glutathione beads alone (*lane 2*), glutathione beads with bovine serum albumin (*lane 3*), prey alone (*lane 4*), and prey with GST-loaded beads (*lane 5*). Some His-Cx43 α 1-CT protein was pulled-down with the bait-loaded beads incubated with prey (*lane 6*), and also in control samples containing either prey alone (*lane 4*), or prey incubated with GST loaded beads (*lane 5*).

FIG. 2. Intracellular accumulation of Cx43 α 1 with N-cadherin knock-down. *A*, cells treated with either N-cadherin siRNAs (*bottom panel*) or control scrambled siRNAs (*upper panel*) were immunostained with an N-cadherin antibody. Note the absence of N-cadherin immunostaining with N-cadherin siRNA treatment (*bottom panel*), whereas in scrambled siRNAs-treated cells, N-cadherin expression remained abundant along cell processes delineating regions of cell-cell contact (see *white arrows*). *B*, Western immunoblotting revealed a reduction in N-cadherin protein abundance in cells transfected with N-cadherin siRNAs, but not with scrambled siRNA or mock-transfected control cells. Using mouse monoclonal P2C4 antibodies, which recognizes predominantly non-phosphorylated Cx43 α 1 (*top panel*) or rabbit polyclonal antibody recognizing all forms of Cx43 α 1 (*bottom panel*), no difference was seen with N-cadherin knock-down in either total Cx43 α 1, or the faster migrating *versus* slower-migrating forms of Cx43 α 1. Tubulin antibody detection served as a loading control. *C*, cells transfected with N-cadherin siRNAs were double-immunostained with antibodies to N-cadherin (*green*) and Cx43 α 1 (*red*). Little or no N-cadherin expression was detected, whereas Cx43 α 1 was localized almost exclusively in the cytoplasm. Scale bar, 25 μ m.



ments, cells were transferred to L-15 medium (with L-glutamine, Invitrogen) and maintained at 37 °C on the heated stage of Leica DM-LFSA microscope equipped with a $\times 40$ objective. Dark field Cy3 imaging was used to locate DsRed-containing cells, and these were dye-injected while being monitored using a FITC filter. Micropipettes were backfilled with 2% 6-carboxyfluorescein, and iontophoretic injection was carried out using 1 nA current pulses of 0.5-s duration at 1 Hz for 1 min. Following injection, a post-impalement DIC image was collected, and passive dye spread was recorded for another 2 min. Dye spread was quantitated by counting total number of dye filled cells and calculating percentage of dye-filled primary neighbors (directly adjacent to injected cell), secondary neighbors (adjacent to primary neighbors), and ternary neighbors (adjacent to secondary neighbors).

Pulse Chase and Cell Surface Biotinylation—Pulse chase experiments were performed as described with minor modifications (28). Cells transfected with Cx43 α 1 or N-cadherin siRNAs were plated on 6-cm tissue culture dishes and incubated for 40 h. Cells were washed twice with phosphate-buffered saline, incubated in Dulbecco's modified Eagle's medium minus methionine for 30 min, followed by labeling with [35 S]methionine (Amersham Biosciences) for 20 min before chase. Biotinylation of cell surface Cx43 α 1 was performed by incubating cells with 1 mg/ml EZ-Link sulfo-NHS-SS-biotin (Pierce) at 4 °C for 30 min. Cx43 α 1 was precipitated from cell lysates using Cx43 α 1 antibody and biotinylated Cx43 α 1 was recovered by streptavidin-coated agarose beads (25).

Time Lapse Videomicroscopy and Motion Analysis—For time lapse videomicroscopy, cells were maintained at 37 °C in L-15 medium supplemented with 10% fetal bovine serum (Hyclone), and visualized using Leica DMIRE2 inverted microscope with a $\times 63$ objective. Images were captured every 2 min over a 1-h interval using an ORCA-ER camera. Motion analysis was carried out using Dynamic Image Analysis Software (Solltech, Inc.) to compute: area, perimeter, roundness ($100 \times 4\pi$

(area/perimeter 2)) (29), speed, directionality (net path length divided by total path length), positive flow (percentage cell area in later images not overlapping earlier image), and negative flow (percentage cell area in earlier image not overlapping later image). Data were analyzed using Student's *t* test with Prism 3 (GraphPad).

RESULTS

Using immunofluorescence microscopy, we examined the distribution of Cx43 α 1 and N-cadherin in NIH3T3 cells. As expected, both proteins are localized in punctate spots at cell-cell contact sites along cell processes. Double immunolabeling with antibodies to Cx43 α 1 and N-cadherin showed regions of cell surface colocalization (Fig. 1 *panel a*). A similar pattern of colocalization was observed for Cx43 α 1 and p120, β -catenin, and ZO-1 (Fig. 1, *panels b–d*). These results indicate a close association between Cx43 α 1, N-cadherin, and N-cadherin-interacting proteins in NIH3T3 cells. This is consistent with the results of previous studies in other cell types (24, 26, 30–36).

Immunoprecipitation and Western immunoblotting experiments were carried out to further characterize the interactions between Cx43 α 1 and N-cadherin (Fig. 1, *panels e and g*). Immunoprecipitations with a Cx43 α 1 antibody followed by Western immunoblotting with a Cx43 α 1 antibody yielded a predominant 43-kDa band, the molecular mass expected for Cx43 α 1 (Fig. 1, *panel g*). Immunodetection using antibodies to N-cadherin, α -catenin, β -catenin, and p120 showed that each of these proteins also coimmunoprecipitated with Cx43 α 1 (Fig. 1, *panel e*). In contrast, immunoblot analysis of

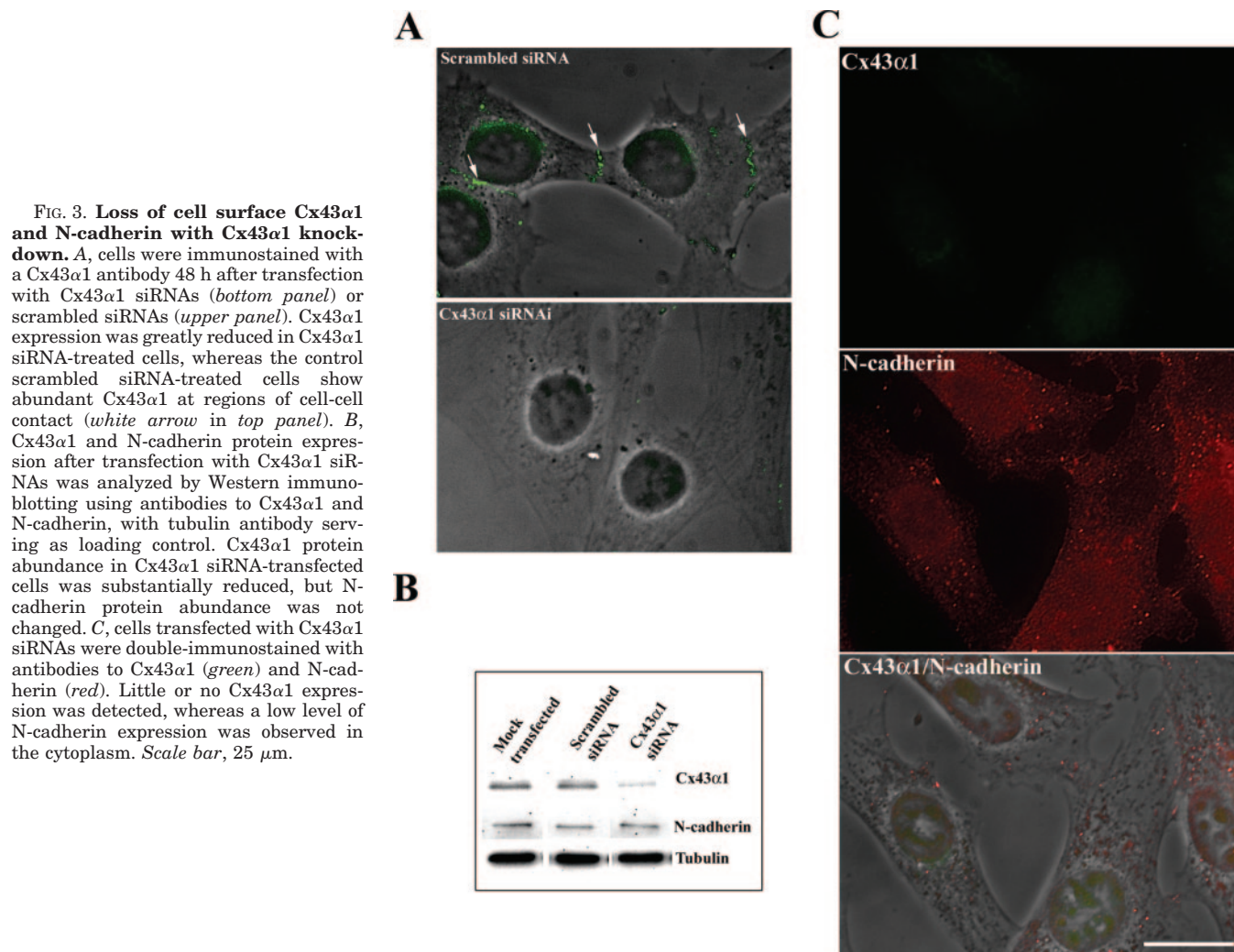


FIG. 3. Loss of cell surface Cx43 α 1 and N-cadherin with Cx43 α 1 knock-down. A, cells were immunostained with a Cx43 α 1 antibody 48 h after transfection with Cx43 α 1 siRNAs (*bottom panel*) or scrambled siRNAs (*upper panel*). Cx43 α 1 expression was greatly reduced in Cx43 α 1 siRNA-treated cells, whereas the control scrambled siRNA-treated cells show abundant Cx43 α 1 at regions of cell-cell contact (*white arrow in top panel*). B, Cx43 α 1 and N-cadherin protein expression after transfection with Cx43 α 1 siRNAs was analyzed by Western immunoblotting using antibodies to Cx43 α 1 and N-cadherin, with tubulin antibody serving as loading control. Cx43 α 1 protein abundance in Cx43 α 1 siRNA-transfected cells was substantially reduced, but N-cadherin protein abundance was not changed. C, cells transfected with Cx43 α 1 siRNAs were double-immunostained with antibodies to Cx43 α 1 (*green*) and N-cadherin (*red*). Little or no Cx43 α 1 expression was detected, whereas a low level of N-cadherin expression was observed in the cytoplasm. Scale bar, 25 μ m.

Cx43 α 1 immunoprecipitates with antibodies to paxillin and focal adhesion kinase (FAK), two proteins found at focal complexes, showed neither proteins were associated with Cx43 α 1 (Fig. 1, *panel f*). To further examine the specificity of the interactions detected in the Cx43 α 1 immunoprecipitates, reciprocal experiments were carried out involving immunoprecipitations using antibodies to either N-cadherin, α -catenin, β -catenin, p120, or ZO-1. This was followed by Western immunoblotting using a Cx43 α 1 antibody (Fig. 1, *panel g*). These studies showed that Cx43 α 1 was indeed coimmunoprecipitated by antibodies to N-cadherin, α -catenin, β -catenin, p120, or ZO-1. Together these results indicate that Cx43 α 1 is localized in a large multiprotein complex containing N-cadherin and many N-cadherin-interacting proteins.

GST and His-tagged Fusion Protein Analyses—To investigate if there is a direct protein-protein interaction between Cx43 α 1 and N-cadherin, we generated fusion proteins for affinity protein binding assays consisting of GST-tagged CT domain of N-cadherin (GST-N-cad-CT) and His-tagged CT domain of Cx43 α 1 (His-Cx43 α 1-CT) (Fig. 1, *panel h*). We focused our analysis on the CT domain of Cx43 α 1, as this region is known to mediate Cx43 α 1 binding of ZO-1 and β -catenin (26, 31–33, 36). Glutathione-agarose beads loaded with GST-N-cad-CT bait were incubated with His-Cx43 α 1-CT prey (Fig. 1, *panel h, lane 6*). Protein bound to the beads were eluted and examined by Western immunoblotting using a His tag antibody. As bait control, His-Cx43 α 1-CT was incubated with glutathione beads loaded with GST (Fig. 1, *panel h, lane 5*),

whereas prey control consisted of glutathione beads incubated with His-Cx43 α 1-CT alone (Fig. 1, *panel h, lane 4*). Additional controls consisted of the glutathione beads alone or glutathione beads incubated with bovine serum albumin (Fig. 1, *panel h, lanes 2 and 3*). Although we found that the GST-N-cad-CT-loaded beads did pull-down a small amount of His-Cx43 α 1-CT fusion protein (Fig. 1, *panel h*), this was also observed in the prey and bait controls (Fig. 1, *panel h, lane 6 versus lanes 4 and 5*). Three independent experiments showed no consistent difference between the experimental *versus* control samples, suggesting that there is little or no specific interaction between the CT domains of Cx43 α 1 and N-cadherin.

To investigate this further, we carried out pull-down assays performed in reverse, *i.e.* with GST-N-cad-CT serving as prey, and His-Cx43 α 1-CT as bait. These studies also showed no direct interaction between the CT domains of Cx43 α 1 and N-cadherin (data not shown). We also performed GST-Cx43 α 1-CT affinity binding assays using total cell lysates as prey, and again found no evidence for N-cadherin binding (data not shown). Finally, Far-Western blotting was carried out using total protein extracts prepared from adult mouse heart, a tissue containing Cx43 α 1 and N-cadherin in abundance. The heart extract was separated by SDS-PAGE, blotted onto a polyvinylidene difluoride membrane, then incubated with GST-Cx43 α 1-CT. Immunodetection with a GST antibody showed no band in the position corresponding to N-cadherin (data not shown). Overall, these experiments suggest no direct interaction between the CT domains of Cx43 α 1 and N-cadherin.

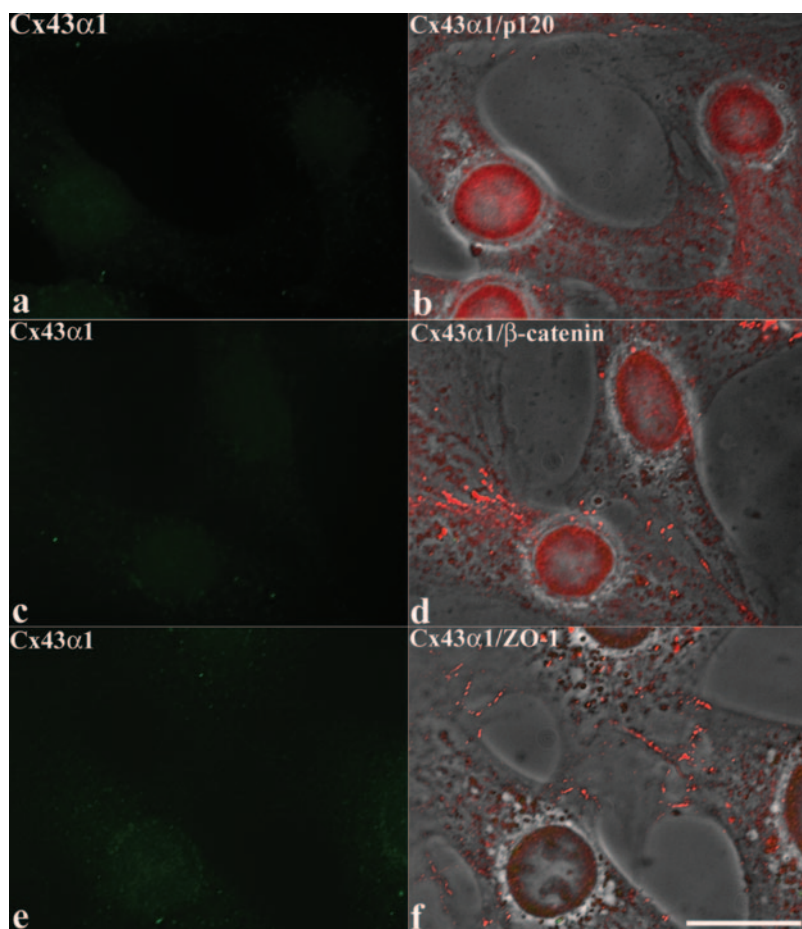


FIG. 4. Cx43 α 1 siRNA treatment alters distribution of N-cadherin-associated proteins. Cells transfected with Cx43 α 1 siRNAs were double-immunostained for Cx43 α 1 (panels a, c, e) and either p120 (panel b), β -catenin (panel d), or ZO-1 (panel f). Cx43 α 1 immunostaining is shown in green and all other antibodies are shown in red. In Cx43 α 1 siRNA-treated cells, little Cx43 α 1 expression was detected. Cell surface expression of p120 (panel b) and β -catenin (panel d) were also greatly reduced or eliminated. In contrast, ZO-1 continued to be expressed abundantly, and was found in small puncta along regions of cell-cell contact (panel f). Note the prominent nuclear localization of p120 as well as some cytoplasmic p120 immunostaining. Scale bar, 25 μ m.

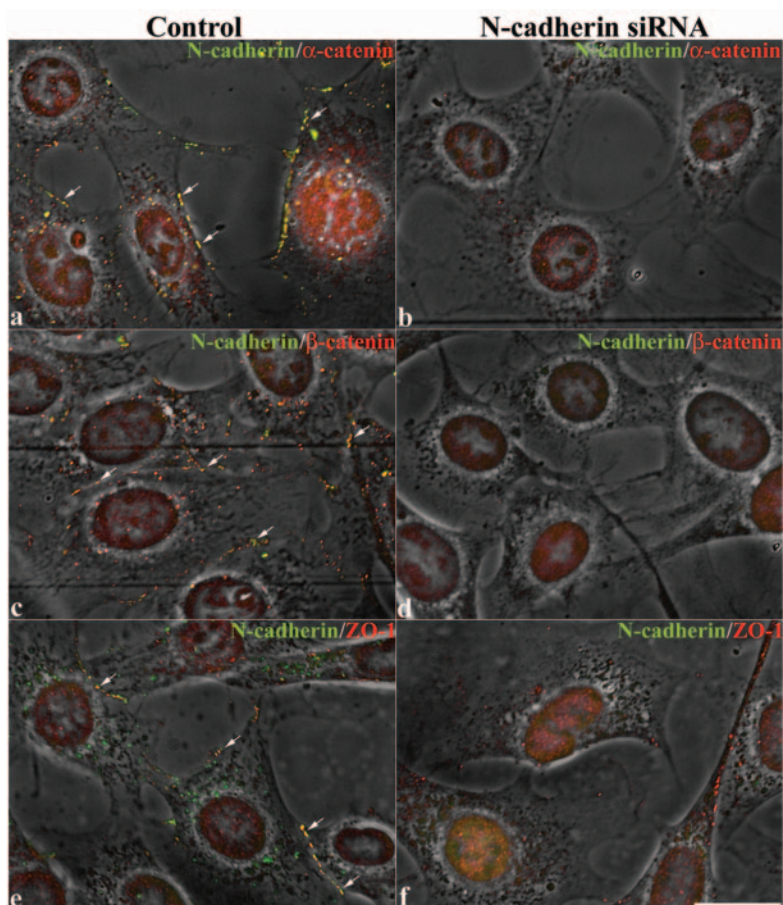


FIG. 5. N-cadherin siRNA treatment alters expression of N-cadherin-associated proteins. Control cells were transfected with scrambled siRNAs and double-immunostained for N-cadherin and N-cadherin-associated proteins, including α -catenin (panel a), β -catenin (panel c), and ZO-1 (panel e). Each of these N-cadherin-associated proteins (red) shows extensive colocalization with N-cadherin (green) at regions of cell-cell contact (yellow puncta denoted by white arrows). In cells transfected with N-cadherin siRNAs, N-cadherin-deficient cells also showed little or no α -catenin (panel b) or β -catenin (panel d) at the cell surface. ZO-1 expression, though persisting, was significantly reduced (panel f). Images were generated by merging the phase contrast and deconvolved darkfield immunofluorescence images. Scale bar, 25 μ m.

siRNA Knockdown of Cx43 α 1 and N-cadherin—We used siRNA knockdown approaches to further evaluate interactions between Cx43 α 1 and N-cadherin. NIH3T3 cells were transiently transfected with two siRNAs targeting different regions of N-cadherin. Such transfected cells showed virtually no detectable N-cadherin when immunostained with an N-cadherin antibody (Fig. 2A). Western immunoblotting showed >80% decrease in N-cadherin protein abundance (top row in Fig. 2B). In contrast, scrambled siRNAs had no effect when compared with control mock-transfected cells (Fig. 2, A and B). Double immunostaining showed that cells depleted of N-cadherin had little or no cell surface Cx43 α 1 immunolabeling, but this was accompanied by a striking intracellular accumulation of Cx43 α 1 (Fig. 2C). Consistent with this, immunoblotting analysis using either a monoclonal antibody (P2C4) that detected predominantly the nonphosphorylated form of Cx43 α 1 (NP) (Fig. 2B, upper panel), or a polyclonal antibody (Sigma) that detected both phosphorylated (PO) and nonphosphorylated Cx43 α 1 (Fig. 2B, lower panel), showed no change in the overall abundance of Cx43 α 1 after N-cadherin siRNA treatment (Fig. 2B).

To determine if the loss of Cx43 α 1 may reciprocally perturb N-cadherin cell surface expression, NIH3T3 cells were transiently transfected with two siRNAs targeting different regions of Cx43 α 1. Immunostaining showed a marked reduction in Cx43 α 1 expression (Fig. 3A), with >80% reduction in Cx43 α 1 protein abundance indicated by Western immunoblotting analysis (Fig. 3B). In contrast, two scrambled siRNAs had no effect (Fig. 3, A and B). When Cx43 α 1 siRNA-treated cells were double-immunostained with Cx43 α 1 and N-cadherin antibodies, N-cadherin was observed predominantly in the cytoplasm in the Cx43 α 1-deficient cells (Fig. 3C). Analysis by Western immunoblotting showed no significant change in N-cadherin protein abundance in the Cx43 α 1 siRNA-treated cells (Fig. 3B). The combined results of these N-cadherin and Cx43 α 1 siRNA studies suggest that the cell surface expression of Cx43 α 1 requires N-cadherin, and conversely, the cell surface expression of N-cadherin also appears to require Cx43 α 1.

Cx43 α 1 siRNA Alters Distribution of N-cadherin-associated Proteins—To determine if Cx43 α 1 knockdown may also affect the distribution of N-cadherin-associated proteins, cells transfected with Cx43 α 1 siRNAs were double-immunostained with antibodies to Cx43 α 1 and p120. Cells deficient in Cx43 α 1 showed a marked reduction in cell surface expression of p120 (Fig. 4, panels a and b), whereas p120 expression in the cytoplasm and nuclei were elevated (compare Figs. 4, panel b with 1, panel b). These results are reminiscent of our previous finding that p120 is redistributed to the nuclei in Cx43 α 1 knockout neural crest cells (24). We also observed with Cx43 α 1 knockdown, the loss of cell surface β -catenin (Fig. 4, panels c and d). A parallel analysis of N-cadherin siRNA-treated cells revealed a similar loss or reduction of cell surface expression of α -catenin, β -catenin, as well as p120 with N-cadherin knockdown (Fig. 5, panels b and d, and data not shown). Despite the overall similarities between the effects of Cx43 α 1 versus N-cadherin siRNA treatment on the reduction in expression of N-cadherin-associated proteins, some differences were noted. Thus Cx43 α 1 siRNA-transfected cells showed the retention of more cytoplasmic β -catenin (Figs. 4, panel d versus 5, panel d), whereas N-cadherin, but not Cx43 α 1 siRNA, caused an apparent reduction in ZO-1 expression (Figs. 4, panel f versus 5, panel f). In control studies carried out with scrambled siRNA treatments, we observed no change in the usual pattern of cell surface colocalization of N-cadherin with α -catenin, β -catenin, and ZO-1 (Fig. 5, panels a, c, and e).

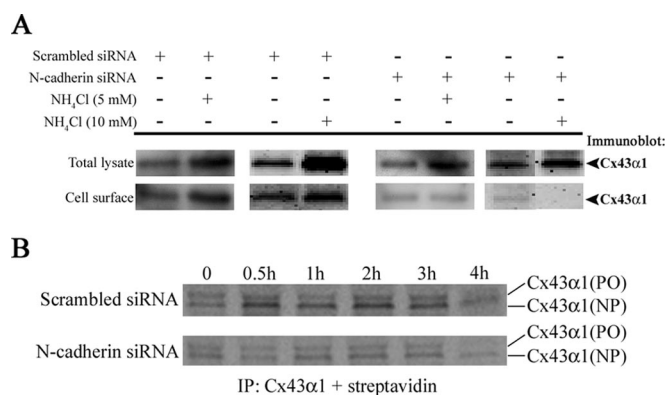


FIG. 6. Lysosomal turnover and cell surface trafficking of Cx43 α 1 in N-cadherin siRNA-transfected cells. A, cells transfected with N-cadherin siRNAs or control scrambled siRNAs were cell surface-biotinylated, lysed, and the cell surface Cx43 α 1 was recovered by immunoprecipitation using streptavidin-coated agarose beads. Some cells were first treated with 5 or 10 mM ammonium chloride, a lysosomal inhibitor, prior to surface biotinylation. In control scrambled siRNA-transfected cells, ammonium chloride treatment elevated total and cell surface localized Cx43 α 1. Untreated N-cadherin siRNA-transfected cells when compared with scrambled siRNA-transfected cells showed a reduction in cell surface expression of Cx43 α 1 even as total Cx43 α 1 expression levels remained unchanged. With ammonium chloride treatment, there was either no change or a small decrease in cell surface expression of Cx43 α 1. B, Cx43 α 1 cell surface trafficking was examined by pulse chase labeling of newly synthesized Cx43 α 1. N-cadherin or scrambled siRNA-transfected cells were labeled with [³⁵S]methionine for 20 min followed by a chase interval of up to 4 h. Surface biotinylated Cx43 α 1 was isolated, and gel separated and blotted, and imaged using a phosphorimager to visualize the cell surface ³⁵S-labeled Cx43 α 1. In scrambled siRNA-treated cells, the Cx43 α 1 bands show strong labeling up to 3 h, with a visible decrease in intensity detected at 4 h. Quantification of the blot provided a half-life estimate of 2.8 h versus 2.3 h for the slower migrating versus faster-migrating species of Cx43 α 1. In the N-cadherin siRNA-treated cells, these Cx43 α 1 bands show only background levels of labeling, with a decrease in intensity also seen at 4 h. The latter may correspond to Cx43 α 1 turnover associated with cells that were not transfected by the N-cadherin siRNA.

Cx43 α 1 Cell Surface Trafficking Inhibited by N-cadherin Knockdown—Our studies showed that Cx43 α 1 expression at the cell surface was largely eliminated by N-cadherin siRNA treatment, but this occurred without any change in total Cx43 α 1 protein abundance. To determine if this discrepancy is because of increased cell surface turnover of Cx43 α 1, or altered cell surface trafficking, we used surface biotinylation to track the cell surface pool of Cx43 α 1. First, we examined Cx43 α 1 expression in N-cadherin siRNA-transfected cells treated with the lysosomal inhibitor, ammonium chloride. Previous studies indicated that Cx43 α 1 turnover can occur via the lysosomal pathway (9, 37, 38). For these studies, lysates were prepared from cells that were surface biotinylated. Using a two-step immunoprecipitation procedure, we first recovered total Cx43 α 1, then secondary immunoprecipitation with streptavidin was carried out to recover the biotinylated cell surface Cx43 α 1. In control scrambled siRNA-transfected cells, total and cell surface localized Cx43 α 1 was increased with ammonium chloride treatment, as would be expected with the inhibition of Cx43 α 1 turnover (Fig. 6A). In the N-cadherin siRNA-transfected cells, the biotinylated cell surface pool of Cx43 α 1 was reduced, in agreement with the reduction in Cx43 α 1 cell surface immunostaining seen with N-cadherin knockdown (Fig. 2C). However, the reduction in cell surface Cx43 α 1 elicited by N-cadherin siRNA treatment occurred with or without ammonium chloride treatment. This would suggest that increased lysosomal turnover cannot account for the reduction in the cell surface pool of Cx43 α 1.

To determine if the reduction in cell surface-localized Cx43 α 1 in N-cadherin-deficient cells is due to altered Cx43 α 1

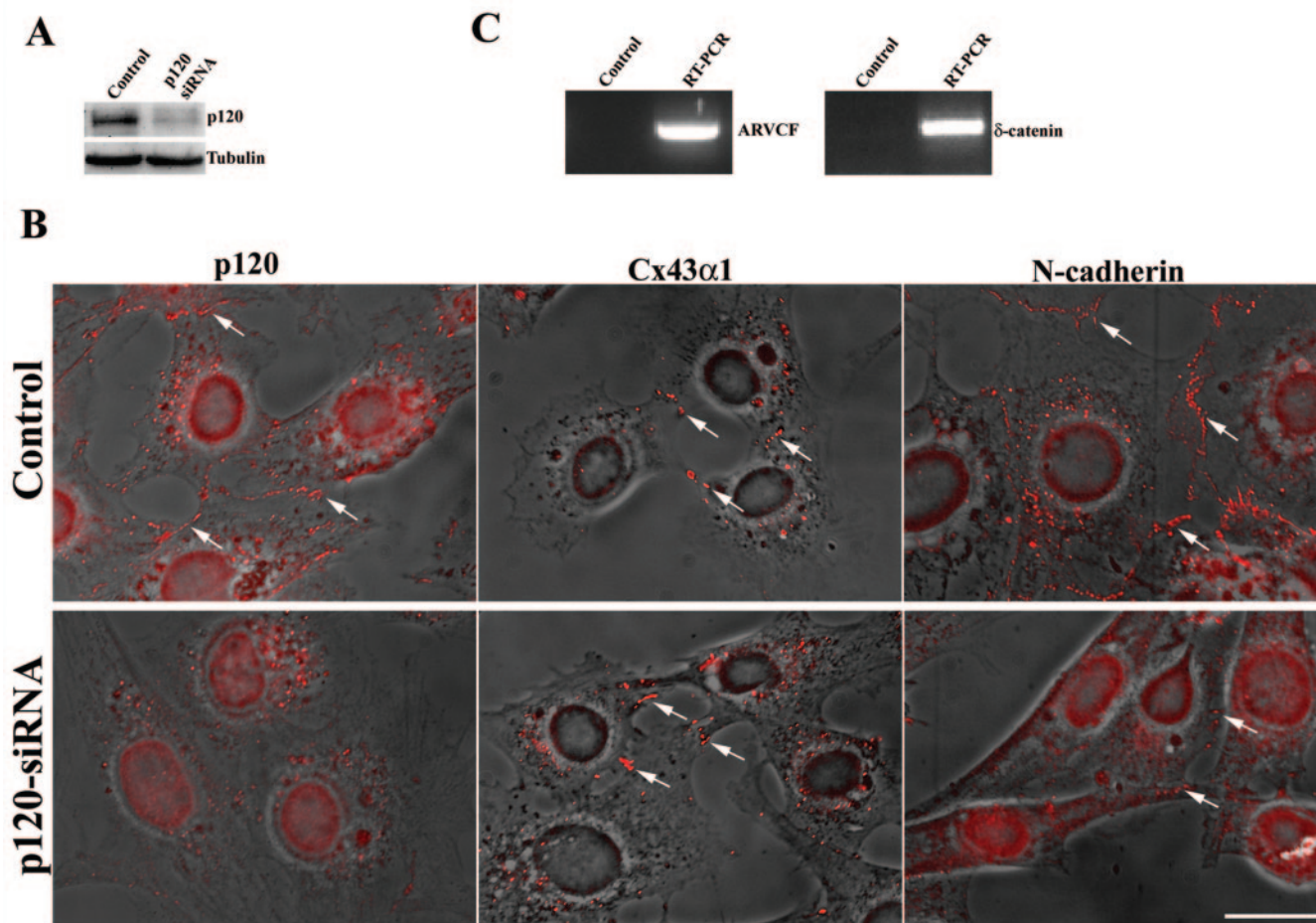


FIG. 7. Differential effects of p120 siRNA knockdown on Cx43 α 1 versus N-cadherin expression. A, Western immunoblot analysis of cells transfected with a p120-siRNA expression vector significant showed a significant decrease in p120 protein abundance. B, cells transfected with p120 siRNA were immunostained with antibodies to p120, Cx43 α 1, or N-cadherin. In control cells, p120 is abundantly expressed at regions of cell-cell contact (*white arrows*), whereas little cell surface expression was seen in p120 siRNA-treated cells. In siRNA-transfected cells, N-cadherin continued to be found at regions of cell-cell contact (*white arrows*), but its abundance was greatly reduced. Surprisingly, Cx43 α 1 expression was unchanged (see *white arrows*). Scale bar, 10 μ m. C, reverse transcriptase-PCR analysis for expression of ARVCF or δ -catenin transcripts in NIH3T3 cells. These assays showed ARVCF and δ -catenin transcripts are both expressed in NIH3T3 cells. Thus a product of the expected size was observed after reverse transcription and PCR amplification with primer pairs for both genes, whereas no products were obtained in the absence of reverse transcriptase (*Control*).

cell surface trafficking, we used pulse chase labeling together with cell surface biotinylation to track the cell surface translocation of newly synthesized Cx43 α 1. For these studies, cells were [35 S]methionine labeled for 20 min, and at timed intervals spanning 4 h, surface biotinylation was carried out followed by harvesting of biotinylated Cx43 α 1. After Western blotting, the radiolabeled biotinylated Cx43 α 1 was then visualized using a phosphorimager. In cells transfected with scrambled siRNA, [35 S]methionine-labeled Cx43 α 1 was detected at the cell surface soon after labeling, but by 4 h, the intensity of labeling was decreased (Fig. 6B, upper panel). This indicates that the pulse-labeled Cx43 α 1 moved off the cell membrane between 3 and 4 h after translocation to the cell surface. This is consistent with previous reports of a half-life of 1–5 h for Cx43 α 1 in cultured cells (for review, see Ref. 6). In contrast, in cells transfected with N-cadherin siRNAs, over the same 4-h chase interval only baseline levels of [35 S]methionine labeling were seen in the cell surface pool of Cx43 α 1. This would suggest that with N-cadherin knockdown, most newly synthesized Cx43 α 1 failed to traffic to the cell surface (Fig. 6B, bottom panel). The observed residual cell surface Cx43 α 1 may represent Cx43 α 1 expression in cells not successfully transfected with the N-cadherin siRNAs. Consistent with this, we note this residual cell surface

Cx43 α 1 band decreased in intensity at 4 h, similar to the profile in control scrambled siRNA-transfected cells and likely reflects normal Cx43 α 1 turnover. Overall, these results indicate that Cx43 α 1 cell surface trafficking is inhibited by N-cadherin knockdown.

N-cadherin Cell Surface Expression Reduced by p120 Knockdown—Several recent studies have indicated that p120 may have an important role in N-cadherin cell surface trafficking and turnover (25, 39). In one study, siRNA-mediated p120 knockdown was shown to eliminate cell surface cadherins by increasing cell surface turnover but without affecting cell surface trafficking of cadherins (25). Using p120-specific siRNAs, we examined the effects of p120 knockdown on N-cadherin and Cx43 α 1 expression in NIH3T3 cells. Western immunoblotting confirmed that p120 siRNA-transfected cells have reduced p120 expression (Fig. 7A). Analysis by immunohistochemistry showed that cells exhibiting p120 knockdown, also exhibited a marked reduction of N-cadherin expression at the cell surface (Fig. 7B). Interestingly, in the p120 siRNA-transfected cells, Cx43 α 1 continued to be expressed abundantly at the cell surface even as N-cadherin expression was reduced (Fig. 7B). Thus in contrast to N-cadherin, Cx43 α 1 cell surface expression does not require p120. To determine if the incomplete elimination of N-cadherin expression by p120 siRNA may reflect functional

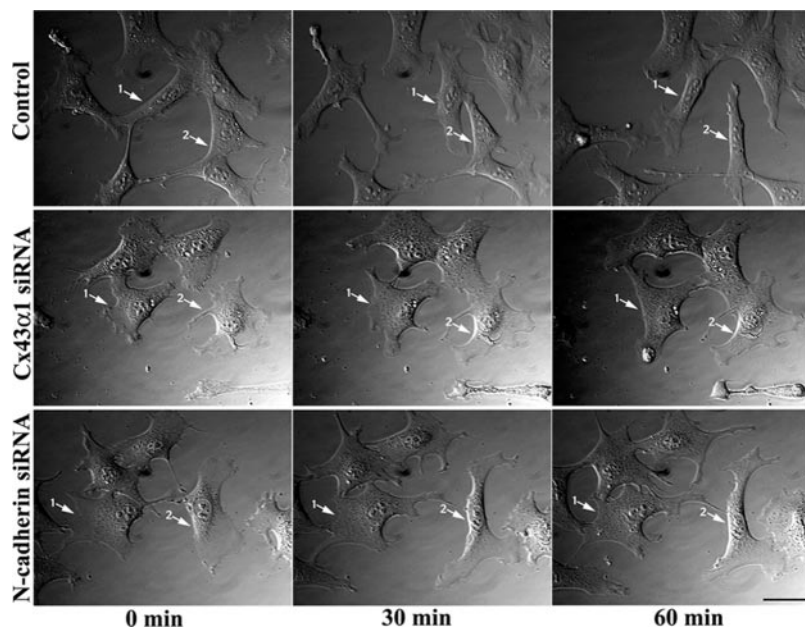
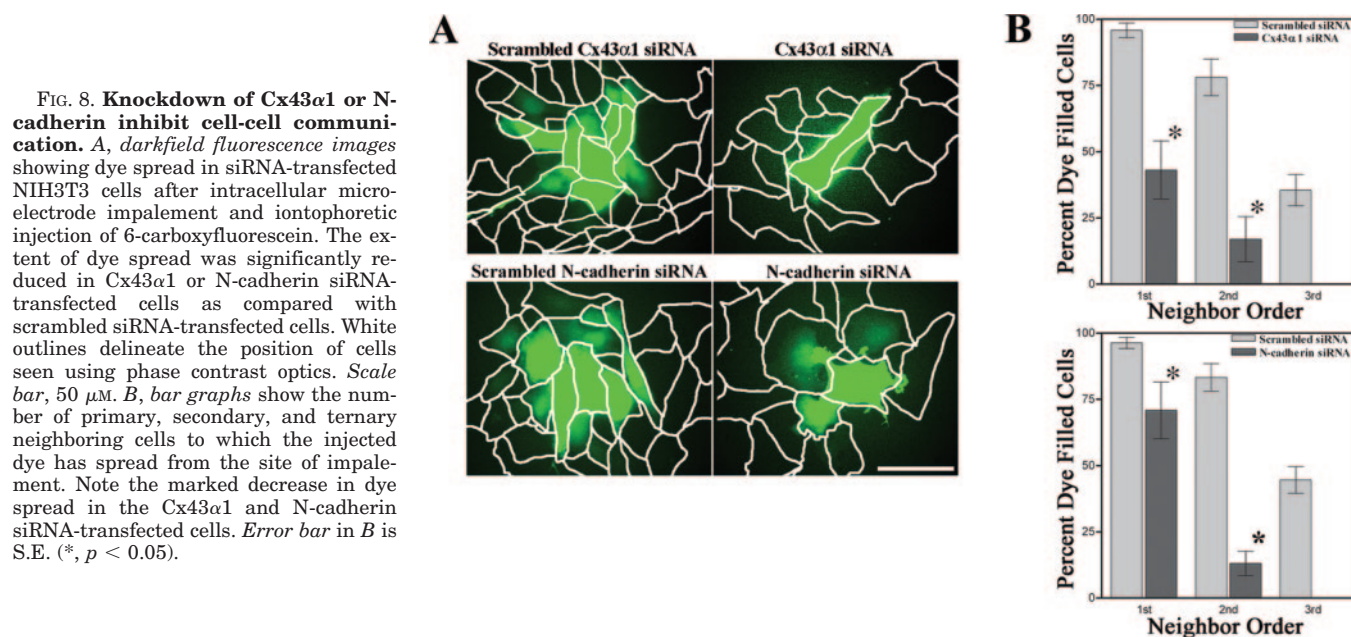


FIG. 9. Time lapse images show reduced cell motility with Cx43 α 1 and N-cadherin knockdown. Cells transfected with EGFP expression vector alone or in combination with Cx43 α 1 or N-cadherin siRNAs were analyzed by time lapse imaging. Shown are phase-contrast images taken at 30-min intervals starting 48 h after siRNA transfection. Cells treated with Cx43 α 1 or N-cadherin siRNAs showed less displacement than control cells (see position of arrows). Scale bar, 25 μ m.

redundancy provided by other p120 family members (25), we used reverse transcriptase-PCR to assay for ARVCF and δ -catenin transcripts, two closely related p120 family members. Indeed transcripts for both were found in NIH3T3 cells (Fig. 7C). Overall, these results are consistent with the demonstrated role of p120 in regulating the cell surface turnover of N-cadherin (25), and they suggest that N-cadherin cell surface turnover may be regulated independently of Cx43 α 1.

Cx43 α 1 and N-cadherin Knockdown Inhibits Gap Junction Communication—To examine the functional consequences of Cx43 α 1 or N-cadherin knockdown, dye coupling was quantitatively assessed in cells transfected with Cx43 α 1 or N-cadherin siRNA. This entailed using intracellular microelectrode impalements to iontophoretically inject the fluorescent dye 6-carboxyfluorescein and monitoring the extent of dye spread (Fig. 8A). Cells transfected with control scrambled Cx43 α 1 siRNAs remained well coupled, with dye spread to 95.8, 78, and 35.5% of primary, secondary and tertiary neighboring cells, respectively (Fig. 8B). In contrast, dye coupling was reduced in cells

transfected with Cx43 α 1 siRNAs ($p < 0.05$), with dye spread seen in only 43.1% of primary neighbors, 17.0% of secondary neighbors, and none of the tertiary neighbors (Fig. 8B). Significantly, cells transfected with N-cadherin siRNAs showed a similar reduction in dye coupling ($p < 0.05$), with dye spread in 70.8% of primary neighbors, 13.1% of secondary neighbors, and 0% of tertiary neighbors, whereas scrambled N-cadherin siRNA-transfected cells remained well coupled (Fig. 8B). These observations suggest that gap junction formation requires the coexpression of Cx43 α 1 and N-cadherin in NIH3T3 cells, in agreement with the results of the immunohistochemical and biochemical analyses.

N-cadherin and Cx43 α 1 Knockdown Inhibits Cell Motility—We also examined the motile behavior of NIH3T3 cells transfected with Cx43 α 1 or N-cadherin siRNA, as previous studies indicated a role for Cx43 α 1 and N-cadherin in modulating cell motility (24, 40, 41). For these studies, cells were transfected with an EGFP expression vector together with siRNA for either Cx43 α 1 or N-cadherin, and the motile behavior of individual

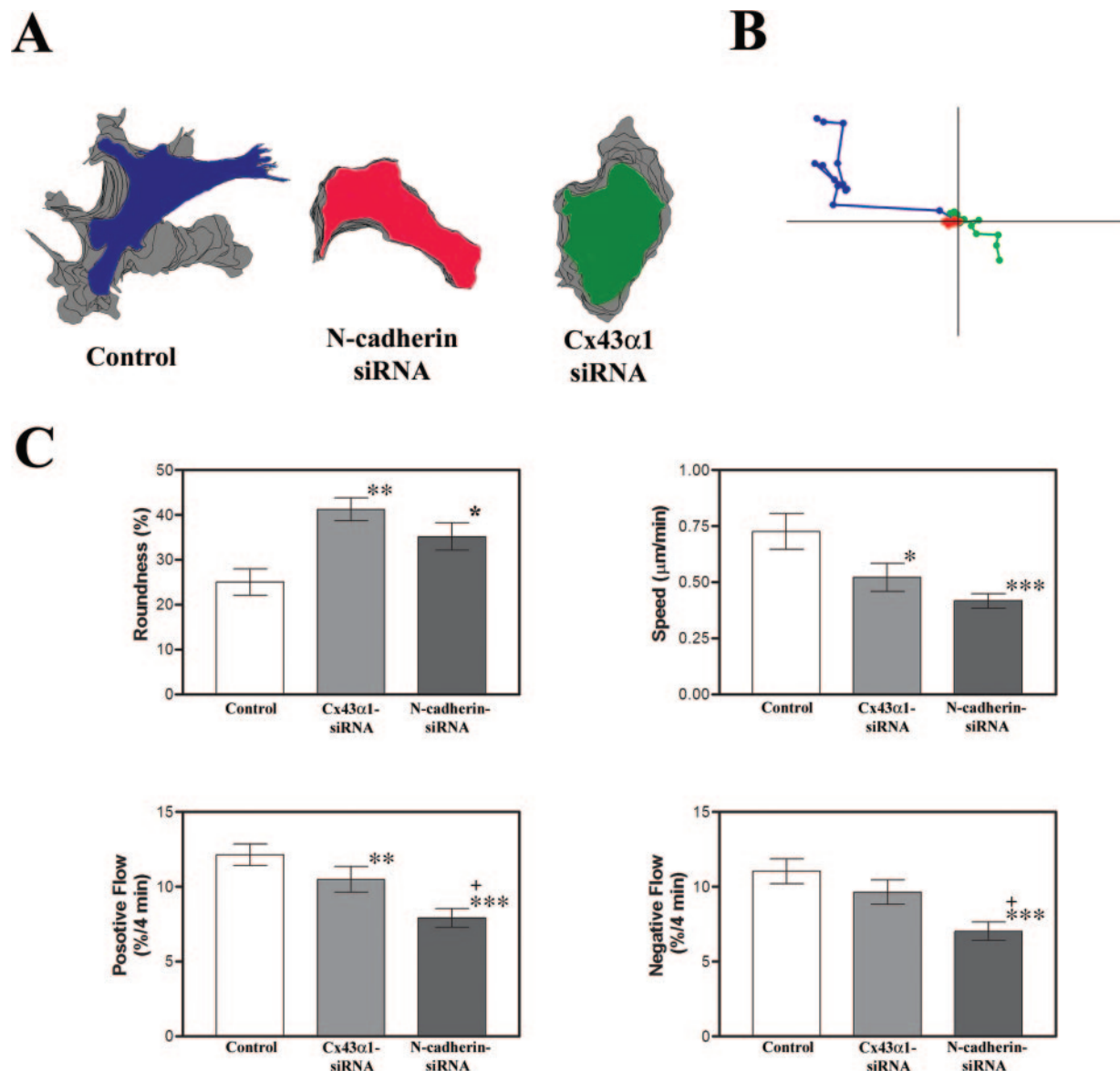


FIG. 10. Motion analysis of cells treated with Cx43 α 1 and N-cadherin siRNA. A, shown are time lapse image stacks obtained from individual control (blue), Cx43 α 1 siRNA (green), and N-cadherin-siRNA (red)-treated NIH3T3 cells captured at 4-min intervals over 1 h. The image on top represents the cell at time 0, with the successive time points indicated by the underlying gray images. Note the much greater net displacement for the control cell, suggesting that N-cadherin or Cx43 α 1 siRNA treatment inhibited cell motility. B, actual migratory paths of the cells shown in A are plotted from a common origin. Much shorter migratory paths were observed for the N-cadherin and Cx43 α 1 siRNA-treated cells as compared with the control cell, indicating a reduction in cell motility with N-cadherin or Cx43 α 1 siRNA treatment. C, effects of siRNA treatment were quantitatively assessed by measuring the roundness of cells, the speed of cell locomotion, and positive and negative cytoplasmic flow. A reduction was observed in the speed of cell locomotion, and in positive/negative flow. In contrast, the roundness of the cells was increased. These findings suggest a reduction in protrusive activity. Error bar in C corresponds to S.E. When compared with control: *, $p < 0.05$; **, $p < 0.01$; ***, $p < 0.005$. When compared with Cx43 α 1 siRNA: +, $p < 0.05$.

cells was examined by time lapse videomicroscopy, with phase contrast and darkfield images captured at 4-min intervals over a period of 1 h. EGFP expression visualized in darkfield images was used to identify cells that are likely cotransfected with the Cx43 α 1 or N-cadherin siRNAs. Control cells showed dynamic changes in cell shape and position, whereas Cx43 α 1 or N-cadherin siRNA-transfected cells exhibited less cell shape changes and little net displacement (Figs. 9 and 10B). Quantitative assessment of cytoplasmic protrusions and retractions, referred to as positive and negative flow, respectively, revealed a reduction in protrusive activity with either Cx43 α 1 or N-cadherin knockdown, but we noted a greater reduction in both positive and negative flow with N-cadherin knockdown (Fig. 10, A and C). Consistent with the reduced protrusive activity, we also found an increase in the round-

ness of the cells, which is calculated from the cell area and perimeter (see "Experimental Procedures," Fig. 10C). With either Cx43 α 1 or N-cadherin siRNA treatment, we also observed a reduction in the overall speed of cell locomotion (Fig. 10C), whereas the directionality of cell movement was unchanged (data not shown). The combined reduction in the speed of cell locomotion and protrusive activity is expected to reduce net cell movement, and this is indeed evident, either by examining the migratory paths of individual cells over the 60-min interval (Fig. 10B), or by comparing the relative cell position in individual time lapse frames (Fig. 9). Overall, these observations show that Cx43 α 1 and N-cadherin siRNA treatment inhibited cell motility in a similar manner, by inhibiting protrusive cell activity and reducing the speed of locomotion.

DISCUSSION

Our study suggests gap junction formation in NIH3T3 cells involve the coassembly of Cx43 α 1 in an N-cadherin containing multiprotein complex. This was indicated by several findings, including immunohistochemistry showing colocalization of Cx43 α 1 with N-cadherin and N-cadherin-interacting proteins, the observation that Cx43 α 1 coimmunoprecipitates with N-cadherin and N-cadherin-interacting proteins, and the finding that siRNA-mediated N-cadherin knockdown resulted in the concomitant loss of cell surface expression of Cx43 α 1. Surface biotinylation experiments showed that this was likely caused by an inhibition in cell surface trafficking of Cx43 α 1. Cx43 α 1 phosphorylation, which was previously shown to be required for Cx43 α 1 gap junction assembly (12, 13, 42), was not altered by N-cadherin knockdown. These results suggest gap junction formation entails a requisite coassembly of connexin and cadherin. Consistent with this, we observed the reciprocal loss of cell surface N-cadherin with siRNA-mediated knockdown of Cx43 α 1. Moreover, dye-coupling studies confirmed that either Cx43 α 1 or N-cadherin knockdown caused a significant reduction in gap junction communication.

Recent studies have indicated that N-cadherin coassembles with catenins in the ER/Golgi compartments prior to its cell surface translocation (43). Interestingly, the forced expression of α -catenin in an α -catenin-deficient prostate cancer cell line has been reported to rescue Cx43 α 1 and Cx32 β 1 trafficking to the cell surface (44). Moreover, targeting of Cx43 α 1 to the plasma membrane in cardiomyocytes have been shown to require the association of Cx43 α 1 with β -catenin and ZO-1 (35). These findings further point to interactions between Cx43 α 1 and N-cadherin/N-cadherin-associated proteins playing a critical role in gap junction formation. However, the precise role of cadherins in gap junction formation may be context or cell-type dependent. Thus in a previous study, the ectopic expression of N-cadherin in L cells was reported to inhibit Cx43 α 1 localization at cell junctions, even as N-cadherin expression in hepatoma cells enhanced gap junction formation (45). Analysis of Cx43 α 1 knockout cardiomyocytes also showed no change in the expression of cadherins and catenins (46), nor were any changes seen in Cx43 α 1 expression in N-cadherin knockout neural crest cells (24). In contrast, N-cadherin knockout cardiomyocytes exhibited significant reductions in the expression of p120, β -catenin, and Cx43 α 1 (18).

We noted some nonreciprocal effects elicited by N-cadherin *versus* Cx43 α 1 siRNA treatment. For example, ZO-1 expression was reduced with N-cadherin knockdown, but not with Cx43 α 1 knockdown. With both N-cadherin and Cx43 α 1 knockdown, cell surface expression of β -catenin was eliminated, but this was accompanied by an accumulation of cytoplasmic β -catenin only with Cx43 α 1 knockdown. These observations suggest a possible hierarchy in interactions between Cx43 α 1, N-cadherin, and N-cadherin-associated proteins. One discrepancy we noted in our studies was that N-cadherin immunostaining was not detected in Cx43 α 1 siRNA-transfected cells even though N-cadherin protein expression was evident in Western immunoblots. We suggest this may reflect a failure of N-cadherin to cluster in Cx43 α 1-deficient cells, making it difficult to detect by immunohistochemistry. This same discrepancy was noted with p120 siRNA knockdown, which disrupted N-cadherin cell surface clustering without affecting total N-cadherin protein expression level (25). A similar situation was previously reported for emerging chick neural crest cells, which showed abundant N-cadherin protein expression by Western immunoblotting but not by immunohistochemistry (47). These observations suggest that perhaps the cell surface clustering of N-cadherin may require both p120 and Cx43 α 1, a possibility that will be further

investigated in future studies. It should be noted that p120 has been shown to play an important role in modulating the cell surface turnover of N-cadherin (25, 39, 48). Our p120 knockdown experiments showed that the loss of p120 expression was accompanied by a reduction in the cell surface expression of N-cadherin, but with no effects on Cx43 α 1 expression. This suggests that N-cadherin turnover may be regulated independently of Cx43 α 1.

We also showed that Cx43 α 1 and N-cadherin knockdown inhibited cell motility. Studies by others have shown that N-cadherin expression can enhance cell motility and also promote tumor metastasis (40, 41). The mechanism by which Cx43 α 1 and N-cadherin modulates cell motility is not known, although it is interesting to note that in Cx43 α 1 knockout neural crest cells and NIH3T3 cells transfected with Cx43 α 1 siRNA, p120 appeared to redistribute from the cell surface to the nucleus (24). Hence, alterations in p120/Rho-GTPase signaling may have a role in mediating cross-talk between the actin cytoskeleton and these two specialized cell junctions (24). Although our studies showed that Cx43 α 1 or N-cadherin knockdown had similar effects on NIH3T3 cell motility, cell protrusive activity was inhibited to a greater extent with N-cadherin knockdown. We previously found that cell motility was inhibited in both N-cadherin and Cx43 α 1 KO neural crest cells, but the precise change in motile behavior differed (24). The basis for the differential effects of Cx43 α 1 *versus* N-cadherin knockdown/knockout on cell motility is not known, but among various possibilities, it could reflect a hierarchical relationship in connexin-cadherin interactions. Together these observations suggest that interactions between connexin and cadherin may play an important role in modulating motile cell behavior.

Overall, these studies indicate that Cx43 α 1 cell surface trafficking and gap junction formation are dependent on the coassembly of Cx43 α 1 in an N-cadherin-containing multiprotein complex. This process of coassembly may account for the close linkage between gap junction and adherens junction formation. Using GST and His-tagged fusion protein binding assays, we found no evidence for direct binding between Cx43 α 1 and N-cadherin, but weak interactions would have been difficult to detect in such *in vitro* assays. The CT domain of Cx43 α 1 protein has been shown to bind proteins such as β -catenin and ZO-1 (26, 31, 33, 36). As the latter proteins also are known to bind N-cadherin, such interactions could serve as a bridge to anchor Cx43 α 1 to N-cadherin-containing protein complexes. As our fusion protein construct included only the CT domain of Cx43 α 1, it leaves open the possibility of interactions mediated by the short N terminus or intracellular loop domains of Cx43 α 1. It is interesting to note that recent studies in *Drosophila* showed that the insect gap junction protein innexin 2 can interact with core proteins in adherens and septate junctions, and likely play an essential role in epithelial morphogenesis (49). Together with our present findings, it would suggest that interactions between connexin and cadherins may be conserved in evolution and may have an important role in regulating cell adhesion, cell-cell communication, and cell motility.

Acknowledgments—We thank P. Lampe for providing antibody reagents and D. Walker for helpful suggestions.

REFERENCES

1. Goodenough, D. A., Goliger, J. A., and Paul, D. L. (1996) *Annu. Rev. Biochem.* **65**, 475–502
2. Kumar, N. M., and Gilula, N. B. (1996) *Cell* **84**, 381–388
3. Sohl, G., and Willecke, K. (2003) *Cell Commun. Adhes.* **10**, 173–180
4. Musil, L. S., and Goodenough, D. A. (1993) *Cell* **74**, 1065–1077
5. Yeager, M., Unger, V. M., and Falk, M. M. (1998) *Curr. Opin. Struct. Biol.* **8**, 517–524
6. Berthoud, V. M., Minogue, P. J., Laing, J. G., and Beyer, E. C. (2004) *Cardiovasc. Res.* **62**, 256–267
7. Musil, L. S., Le, A. C., VanSlyke, J. K., and Roberts, L. M. (2000) *J. Biol. Chem.* **275**, 25207–25215

8. Laing, J. G., and Beyer, E. C. (1995) *J. Biol. Chem.* **270**, 26399–26403
9. Laing, J. G., Tadros, P. N., Westphale, E. M., and Beyer, E. C. (1997) *Exp. Cell Res.* **236**, 482–492
10. Herve, J. C., Plaisance, I., Loncarek, J., Duthe, F., and Sarrouilhe, D. (2004) *Eur. Biophys. J.* **33**, 201–210
11. Lampe, P. D., and Lau, A. F. (2004) *Int. J. Biochem. Cell Biol.* **36**, 1171–1186
12. Musil, L. S., and Goodenough, D. A. (1991) *J. Cell Biol.* **115**, 1357–1374
13. Musil, L. S., Cunningham, B. A., Edelman, G. M., and Goodenough, D. A. (1990) *J. Cell Biol.* **111**, 2077–2088
14. Laird, D. W., Puranam, K. L., and Revel, J. P. (1991) *Biochem. J.* **273**, 67–72
15. Frenzel, E. M., and Johnson, R. G. (1996) *Dev. Biol.* **179**, 1–16
16. Keane, R. W., Mehta, P. P., Rose, B., Honig, L. S., Loewenstein, W. R., and Rutishauser, U. (1988) *J. Cell Biol.* **106**, 1307–1319
17. Meyer, R. A., Laird, D. W., Revel, J. P., and Johnson, R. G. (1992) *J. Cell Biol.* **119**, 179–189
18. Luo, Y., and Radice, G. L. (2003) *J. Cell Sci.* **116**, 1471–1479
19. Hertig, C. M., Eppenberger-Eberhardt, M., Koch, S., and Eppenberger, H. M. (1996) *J. Cell Sci.* **109**, 1–10
20. Lee, S., Gilula, N. B., and Warner, A. E. (1987) *Cell* **51**, 851–860
21. Paul, D. L., Yu, K., Bruzzone, R., Gimlich, R. L., and Goodenough, D. A. (1995) *Development* **121**, 371–381
22. Li, W. E., Waldo, K., Linask, K. L., Chen, T., Wessels, A., Parmacek, M. S., Kirby, M. L., and Lo, C. W. (2002) *Development* **129**, 2031–2042
23. Huang, G. Y., Cooper, E. S., Waldo, K., Kirby, M. L., Gilula, N. B., and Lo, C. W. (1998) *J. Cell Biol.* **143**, 1725–1734
24. Xu, X., Li, W. E., Huang, G. Y., Meyer, R., Chen, T., Luo, Y., Thomas, M. P., Radice, G. L., and Lo, C. W. (2001) *J. Cell Biol.* **154**, 217–230
25. Davis, M. A., Ireton, R. C., and Reynolds, A. B. (2003) *J. Cell Biol.* **163**, 525–534
26. Toyofuku, T., Yabuki, M., Otsu, K., Kuzuya, T., Hori, M., and Tada, M. (1998) *J. Biol. Chem.* **273**, 12725–12731
27. Brummelkamp, T. R., Bernards, R., and Agami, R. (2002) *Science* **296**, 550–553
28. Fujita, Y., Krause, G., Scheffner, M., Zechner, D., Leddy, H. E., Behrens, J., Sommer, T., and Birchmeier, W. (2002) *Nat. Cell Biol.* **4**, 222–231
29. Stites, J., Wessels, D., Uhl, A., Egelhoff, T., Shutt, D., and Soll, D. R. (1998) *Cell Motil. Cytoskeleton* **39**, 31–51
30. Barker, R. J., Price, R. L., and Gourdie, R. G. (2001) *Cell Commun. Adhes.* **8**, 205–208
31. Barker, R. J., Price, R. L., and Gourdie, R. G. (2002) *Circ. Res.* **90**, 317–324
32. Giepmans, B. N., and Moolenaar, W. H. (1998) *Curr. Biol.* **8**, 931–934
33. Giepmans, B. N., Verlaan, I., and Moolenaar, W. H. (2001) *Cell Commun. Adhes.* **8**, 219–223
34. Postma, F. R., Hengeveld, T., Alblas, J., Giepmans, B. N., Zondag, G. C., Jalink, K., and Moolenaar, W. H. (1998) *J. Cell Biol.* **140**, 1199–1209
35. Wu, J. C., Tsai, R. Y., and Chung, T. H. (2003) *J. Cell. Biochem.* **88**, 823–835
36. Ai, Z., Fischer, A., Spray, D. C., Brown, A. M., and Fishman, G. I. (2000) *J. Clin. Investig.* **105**, 161–171
37. Laing, J. G., Tadros, P. N., Green, K., Saffitz, J. E., and Beyer, E. C. (1998) *Cardiovasc. Res.* **38**, 711–718
38. Jordan, K., Chodock, R., Hand, A. R., and Laird, D. W. (2001) *J. Cell Sci.* **114**, 763–773
39. Chen, X., Kojima, S., Borisy, G. G., and Green, K. J. (2003) *J. Cell Biol.* **163**, 547–557
40. Hazan, R. B., Phillips, G. R., Qiao, R. F., Norton, L., and Aaronson, S. A. (2000) *J. Cell Biol.* **148**, 779–790
41. Nieman, M. T., Prudoff, R. S., Johnson, K. R., and Wheelock, M. J. (1999) *J. Cell Biol.* **147**, 631–644
42. Cooper, C. D., and Lampe, P. D. (2002) *J. Biol. Chem.* **277**, 44962–44968
43. Wahl, J. K., 3rd, Kim, Y. J., Cullen, J. M., Johnson, K. R., and Wheelock, M. J. (2003) *J. Biol. Chem.* **278**, 17269–17276
44. Govindarajan, R., Zhao, S., Song, X. H., Guo, R. J., Wheelock, M., Johnson, K. R., and Mehta, P. P. (2002) *J. Biol. Chem.* **277**, 50087–50097
45. Wang, Y., and Rose, B. (1997) *J. Cell Sci.* **110**, 301–309
46. Gutstein, D. E., Liu, F. Y., Meyers, M. B., Choo, A., and Fishman, G. I. (2003) *J. Cell Sci.* **116**, 875–885
47. Monier-Gavelle, F., and Duband, J. L. (1995) *J. Cell Sci.* **108**, 3839–3853
48. Xiao, K., Allison, D. F., Buckley, K. M., Kottke, M. D., Vincent, P. A., Faundez, V., and Kowalczyk, A. P. (2003) *J. Cell Biol.* **163**, 535–545
49. Bauer, R., Lehmann, C., Martini, J., Eckardt, F., and Hoch, M. (2004) *Mol. Biol. Cell* **15**, 2992–3004